# Fault diagnosis of a photovoltaic system using recurrent neural networks

**Reda Djeghader, Ilyes Louahem Msabah, Samia Benzahioul, Abderrezak Metatla**
Department of Mechanical Engineering, Faculty of Technology, University of Skikda, Skikda, Algeria

## Article Info

## ABSTRACT

The developed work in this paper is a part of the detection and identification of faults in systems by modern techniques of artificial intelligence. In a first step we have developed amulti-layer perceptron (MLP), type neural network to detect shunt faults and shading phenomenon in photovoltaic (PV) systems, and in the second part of the work we developed anotherrecurrent neural network (RNN) type network in order to identify single and combined faults in PV systems. The results obtained clearly show the performance of the networks developed for the rapid detection of the appearance of faults with the estimation of their times as well as the robust decision to identify the type of faults in the PV system.

*Corresponding Author:*

Reda Djeghader
Department of Mechanical Engineering, Faculty of Technology, University of Skikda
BP 26 Route El-hadaîak, Skikda, Algeria
Email: r.djeghader@univ-skikda.dz

## 1. INTRODUCTION

In the work developed by Chen *et al.* [1], an intelligent technique of optimization and fault diagnosis called nelder mead simplex (NMS) is used for the improvement of the reliability of photovoltaic (PV) plants based on the optimization of parameters by a learning algorithm called Kernel based external learning machine (KELM) which affects defect classification performance in PV. Bouselhama *et al.* [2] presented a new technique of maximum power point tracking (MPPT) of a partially shaded PV system based on an artificial neural network, this technique is a combination of artificial neural networks with a scanning algorithm to get the MPPT. Chen *et al.* [3] developed a technique for locating faults in a PV string based on a sliding window of a time series sliding window (TSSW) time series where they calculated the local external factor (LOF) for each point of the current in TSSW, and this factor exceeded the threshold value c which indicates that this series is in a state of failure, they have proved that this technique is effective in detecting faults in the PV system. Research by Belaout *et al.* [4] a multi-layered adaptive neural fuzzy classifier was developed in order to detect and classify the defects in the PV network by combining two types of fuzzy neuron network. They deduced that the multiclass adaptive neuro-fuzzy classifier (MCNFL) network is more precise than that of the artificial neuron network (ANN) alone. Hachanaa *et al.* [5] used a real test bench with different operating scenarios and presented it mathematically to analyze the effects of faults from the intermediary of the I-V characteristic.

A fault diagnosis strategy in the inverter/PV string system has been developed by Spataru *et al.* [6], to detect the shading phenomenon and the increase in series resistance losses as well as the degradation induced by the potential affecting the PV chain based on the changes in the I-V characteristic.

In this paper we have developed a work that is a part of the detection and identification of faults in the PV system. The detection step is based on the use of a multi-layer perceptron (MLP) type network in order to detect the appearance of faults and the estimation of their times. For the identification step we have developed another network of the RNN recurrent type to identify and isolate the faults.

## 2.    DESCRIPTION OF THE PV SYSTEM

In the first part of the description of the used system, we study two types of faults in a PV system. The PV system under study is a PV field which comprises (03) three strings in parallel, each string contains (03) three modules in series and each one contains (60) sixty poly-crystalline cells. A database has been created which expresses the different operating modes of the PV system. The first scenario expresses the operating state of the healthy system with 1529 test, and then an operation with the presence of shading phenomenon with 657 experiments and the last operating mode shows those of the presence of faults of resistance with 124 experiments. Table 1 illustrates a description of the database used in the study [5], [6]. In the second part of the work we presented a study on the detection and identification of faults of single and combined sensors in the PV system defined previously with different instants and amplitudes. Table 2 shows the appearance of physical faults and their influences on the strings at different times.

Table 1. Description of PV system database

| Status of PV | Number of experiments | Causes and effects |
|---|---|---|
| Healthy state | 1529 | Optimal operation of the PV system |
| Shading problem | 657 | Causes a low generated voltage and a low power |
| Resistance fault | 124 | Degradation of interconnections cracking corrosion of inter-cell links, is related to the problem of increasing the resistance of the connection between two PV modules |
| Total | 2310 | |

Table 2. Description of physical faults and their influences on the strings

| Scenarios | No string | Fault type | | Time of fault (k) |
|---|---|---|---|---|
| | | Shading | Shunt | |
| 1st | String1 | | + | 100 |
| 2nd | String2 | + | | 100 |
| 3rd | String3 | + | | 100 |
| 4th | String1 | + | | 100 |
| | String2 | + | | 100 |
| 5th | String1 | | + | 100 |
| | String2 | + | | 100 |

## 3.    PV SYSTEM MODELING

Figure 1 shows a PV field used in the study, this field has three strings in parallel, each string contains three modules in series. The latter consists of sixty (60) poly-crystalline cells [7]. The one-diode PV generator (PVG) model will be adopted, the equivalent electric circuit is shown in Figure 2 [8]–[12]. The mathematical model of the PV string used in the study is shown in the following part [13]–[16]:

$$I = I_{ph} - I_0 \times (exp(\frac{V - I \times R_s}{V_t}) - 1) - \frac{V - I \times R_s}{R_{sh}} \tag{1}$$

Where T is temperature; G is solar irradiance; $I$ is current supplied by the cell [A]; $V$ is voltage at the cell terminal [V]; $I_{ph}$ is equivalent current proportional to the sunshine received by the cell; $I_0$ is reverse saturation current of the diode; $V_t = \frac{a.k_b.T_c}{q}$ is thermal voltage of the diode. It depends on the temperature of the $T_c$ cell. While, $a, k_b$ and $q$ are respectively the diode ideality factor (1 to 2), the Boltzmann constant (1.38 10-23 J/°K) and the electron charge (1.602 10-19 C); $R_s$ isseries resistance of the cell; $R_{sh}$ is shunt resistance of the cell.
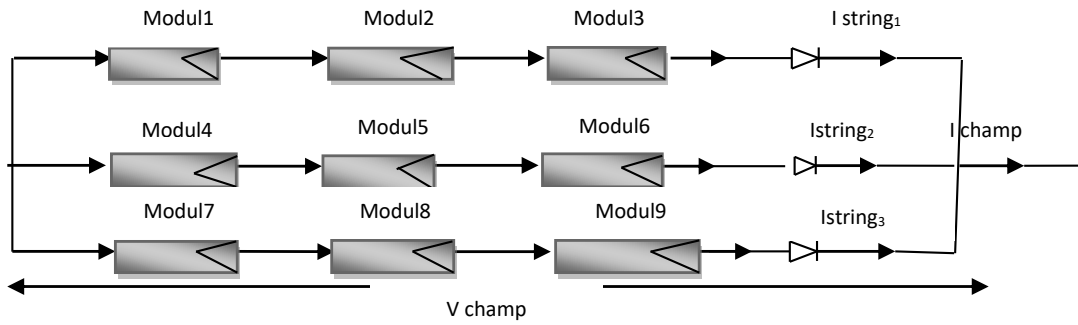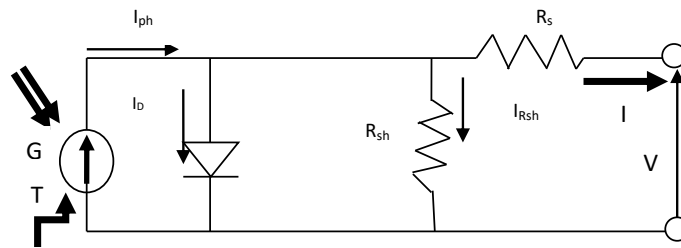
Figure 1. The configuration of the PV field studies



Figure 2. Equivalent diagram of a model PV cell with one diode

## 4.     PROPOSED METHOD

In this part of the work, we have presented the methodology of detection and identification of faults in the PV system. It is based on a two step neural network procedure: a first neural network is used for residual generation and a second recurrent neural network performs residual evaluation. As illustrated in the Figure 3.
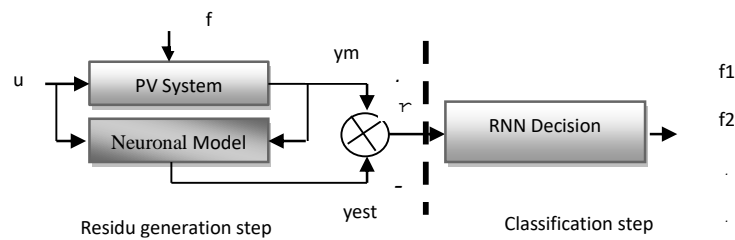


Figure 3. Principle of isolation and classification of faults

### 4.1.  Residue generation step

First, we presented a step of detection by the generation of residuals based on a comparison of the real output of the system and that estimated from a neuronal model of the neural network auto-regressive exogenous (NNARX) input type by the learning method of Levenberg-Marquatdt [17], [18]. The basic principle of this neural model is presented by the flowchart in Figure 4. The generation of residues by the method developed in our work goes through the following steps (see Figure 4). The first step is to collect a set of data describing the behavior of the PV system. The idea is to vary the inputs u(t) and estimate the outputs y(t) to obtain a dataset as shown by the following formulation:

$$Z^N = \{(u(t), y(t)), \quad t = 1, \ldots, N\} \tag{2}$$

Where $Z$ is all the data of the experimental base; $u(t)$ is input vector; $y(t)$ is output vector; $N$ is dimension of the database.
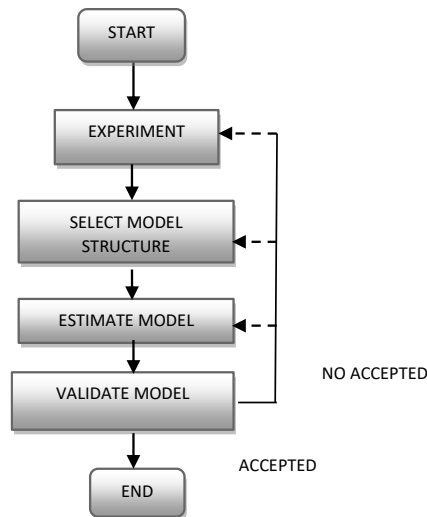
Figure 4. Residue generation flowchart

If the system to be identified is unstable, or contains marginally stable dynamics (slightly damped), it is necessary to perform a closed loop experiment to improve the output estimation based on a good choice of the sampling frequency, with a suitable input signal and data preprocessing.

### 4.1.1. Selecting the model structure

The next step is to choose an optimal model of nonlinear structure in (3):

$$\hat{y}(k) = g(\varphi(k), \theta) \tag{3}$$

Where $\varphi(k)$ is a vector containing the regressors, $\theta$ is a vector containing the weights and $g$ is the function realized by the neural network. The NNARX model is recommended [17], [18] when the considered system is deterministic or weakly noisy and the model is defined by the regression vector:

$$\varphi(t) = [y(t-1)\dots y(t-n_a) \quad u(t-n_k)\dots u(t-n_b-n_k+1)]^T \tag{4}$$

### 4.1.2. Model estimation

When a set of candidate models is chosen, we take the one that gives the best prediction by minimizing the error, in the sense of least squares, between the observed outputs and the predictions (or according to another type of criterion). From a statistical point of view this procedure is called estimation, whereas in the neural context it is called learning.

### 4.1.3. Validation

When this model is estimated or trained, it must be evaluated to see whether or not it meets the set requirements. If the model is not validated, we go back to one of the previous steps. The generation of residues was determined as in (5).

$$y_m(t) - y_{est}(t) = r(t) \tag{5}$$

Where $y_m(t)$ is actual system output, $y_{est}(t)$ is estimated output and $r(t)$ is identification residuals. The calculated residuals are used to build a database of residuals to be highlighted for the training of another neural-like decision algorithm (levenberg-Marquatdt).

### 4.2. Identifaction step

Another step of identification and isolation of defects was carried out by an RNN neural model of retro-propagation type algorithm, the basic principle of this neural model is presented by [17]–[19] it is carried out according to the steps as follows: i) initialize the MLP neuron network weights $W_{ij}$ with small random values, ii) present a training repository of our algorithm to calculate the prediction errors and the estimated output, iii) calculate the partial derivatives of the error with respect to each weight and adjust the

network parameters, and iv) resetting the operation until it reaches the desired output value. The principle of this network is presented in Figure 5 [19]–[25]. The chosen recurrent network (RNN) is made up of three layers. The input layer contains the residuals and the delayed decisions, the hidden layer whose number of neurons is determined empirically, and the output layer contains the fault indicators. The corresponding NNARX networks is then described by:

$$D(c_i) = \varphi_i(Z * h_i + z_0) \tag{6}$$

or:

$$h_i = \varphi_i(w * x_i + w_0) \tag{7}$$

Where $D(c_i)$ is ith decision function; $Z$ is matrix of weights connecting the neurons of the hidden layer to those of the output layer; $z_0, w_0$ is the bias vectors; $\varphi$ is represents the sigmoid function which transforms the interval $[-\infty, +\infty]$ into $[0,1]$; $h_i$ is represents the output of the hidden layer; $w$ is matrix of weights connecting the neurons of the hidden layer to those of the input layer; $x_i$ is represents the stimulus (the input to the RDN) which is the residues and previous decisions.
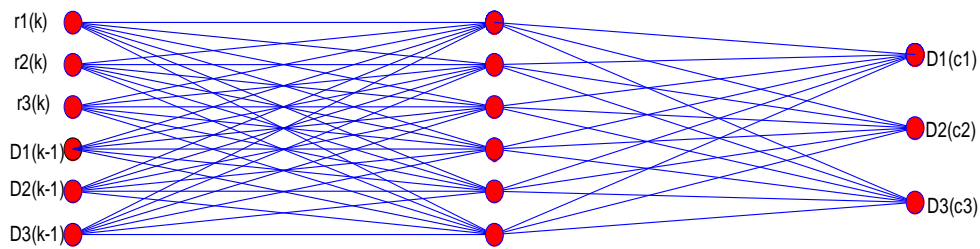


Figure 5. RNN used for residual evaluation

## 5. RESULTS AND DISCUSSION

Figure 6 represent respectively the temperature and the solar radiation of the PV system studied in the healthy case and with the phenomenon of shading. According to the curves Figure 6 we see that, the phenomenon of shading is very clear on the evolution of the temperature and the sunshine as a function of time compared to the evolution of the two characteristics in the case of absence of shading. Figure 7 represent the evolution of the output currents of the PV system in the normal cases, shading and with a resistance fault. According to the first curve of the Figure 6 we see that, the evolution of current generated by the PV system in the shaded case decreases to the lower value of 2 A compared to the normal case which varies around 5 A and shows the effect of shading phenomenon on the current generated by the PV system and consequently on the power supplied by the PV system. However, the evolution of the tension in the two cases is almost identical.
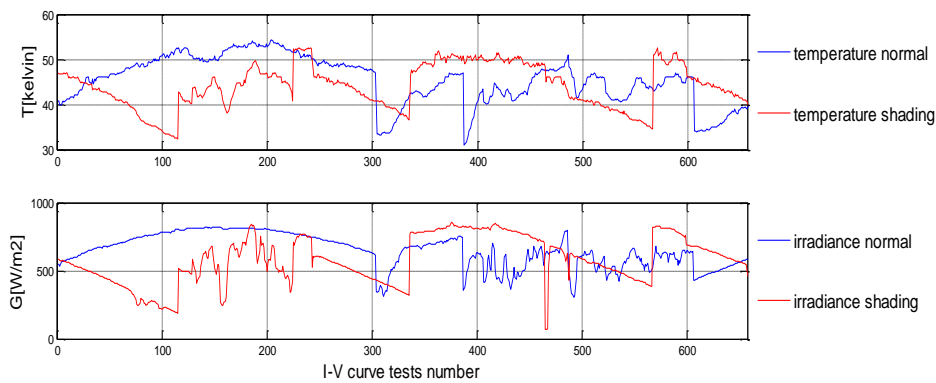


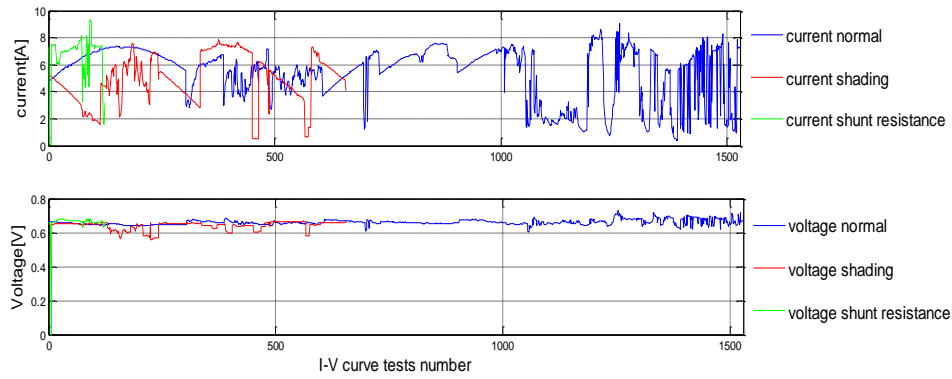Figure 6. Temperature and sunshine in normal cases and with shading phenomenon

Figure 7. Current as a function of the number of tests I-V good case, shading and resistance defect

Figure 8 show the I-V and P-V characteristics of the studied PV system in the three operating normal modes, shaded and with the presence of resistance faults. The I-V & P-V characteristics of the PV system show that, the maximum operating point (MPP) in the shaded case is different from that of the normal case. However, the case of faults resistance slightly different from that of the value of MPP in normal case, which shows that the MPP is more sensitive to the phenomenon of shading has that of defects of resistance.
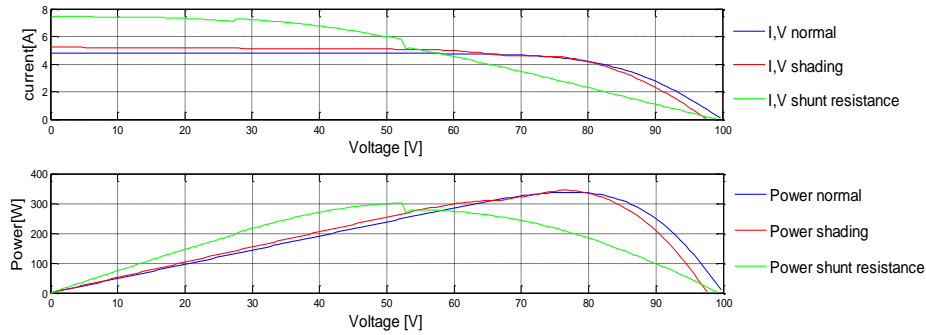


Figure 8. PV system I-V & P-V characteristics with the three operating modes

### 5.1. Residual generation

Before starting the steps of detection and identification of faults, we performed computational tests in Matlabenvironment to show the robustness and precision as well as the speed of the neural network developed in order to estimate the output of MLP-type PV system with an NNARX neural model based on the learning algorithm (Levenberg-Marquardt), the latter contains 13 input and 3 output neurons with a single hidden layer of 13 neurons, their activation functions of hyperbolic tangent type (TH). Figure 9 shows the estimated and real currents with their string 1 prediction error. Figures 10 and 11 shows the estimated and actual currents as well as the string 2 prediction error.
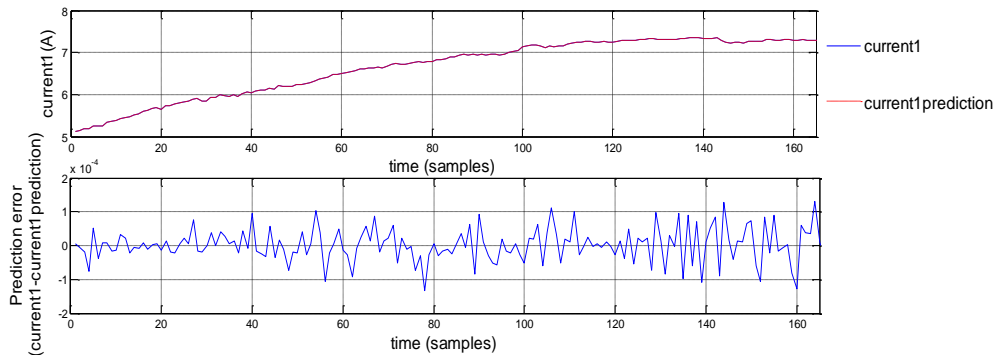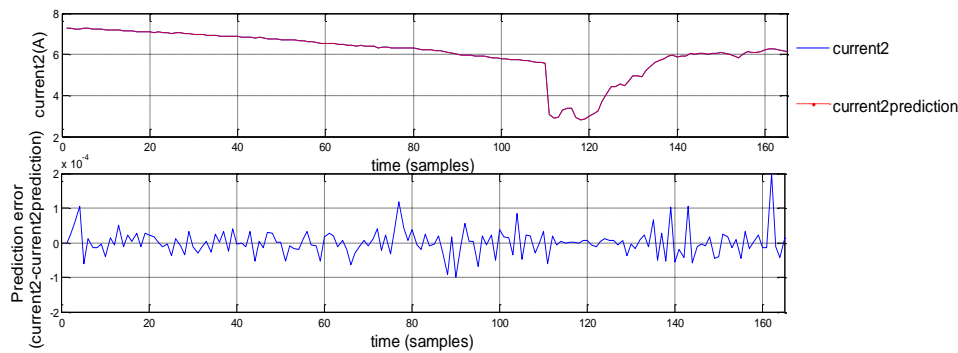


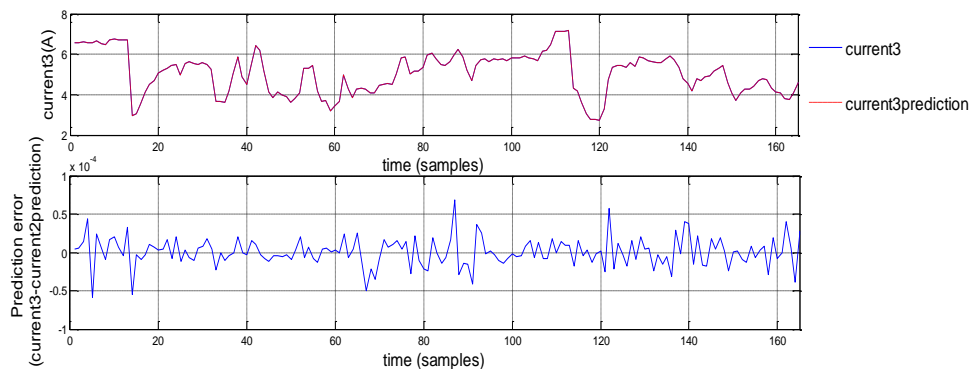Figure 9. String sizes 1

Figure 10. String sizes 2



Figure 11. String sizes 3

The obtained computation results show that, the currents at the level of the three strings take an identical amplitude in the three cases with a small change during their evolutions with time, this change one with respect to the other probably due to the position of the three strings in relation to the sunshine, the quadratic error used stabilizes at a value of $10^{-5}$ at the level of iteration number 1417, this value is considered a good estimate in terms of precision and response time.

### 5.2.  Detection and identification steps

### 5.2.1. Case of a normal system

In this part of the work we have developed another RNN neural network with a learning algorithm for the identification of physical faults in the PV system. Figure 12 show the identification residues of the three flawless strings. We see that the residuals of the three strings with an amplitude of $2 \times 10^{-4}$ for the two first strings and the third string with an amplitude of $1 \times 10^{-4}$, with a quadratic error stabilizes at the value of $10-6$ with 300 iterations (Epochs) and the decision of the neural network used tends towards zero in the case of strings without defects.

### 5.2.2. Simple default

In this first part, we presented the case of simple physical faults (shading phenomenon or shunt fault) at the PV system string level.
- Shunt fault

The results obtained in Figure 13 show the identification residuals with the decision of RNN neural network with the presence of shunt faults in the PV system at the level of strings 1 to 100. The identification residues obtained in this case show that the first residue corresponds to string I of the PV system, the latter indicates the presence of a fault of absolute amplitude of 5.7 A at the 100 samples. This presence of fault is confirmed by the decision of the neural network with a logical response of one (1) in the string I to the 100 samples and zero in the other two strings 2 and 3.
- Case of shading phenomenon

The obtained results in Figure 14 show the identification residues with the decision of the RNN neural network in the presence of the shading phenomenon in the PV system at the second-string level from

time 100.The obtained identification residues in this case show that the second residue corresponds to string II of the PV system, the latter indicates the presence of a defect from 100 samples (k) this defect with an amplitude residue at the beginning reaches 5.2 A, and from 160 samples stabilizes around 1.5 A. The used RNN network decision confirmed the presence of a fault from sample number 100, the logical decision equals 1 at the level of string II tends to 0 in the other string I and III.
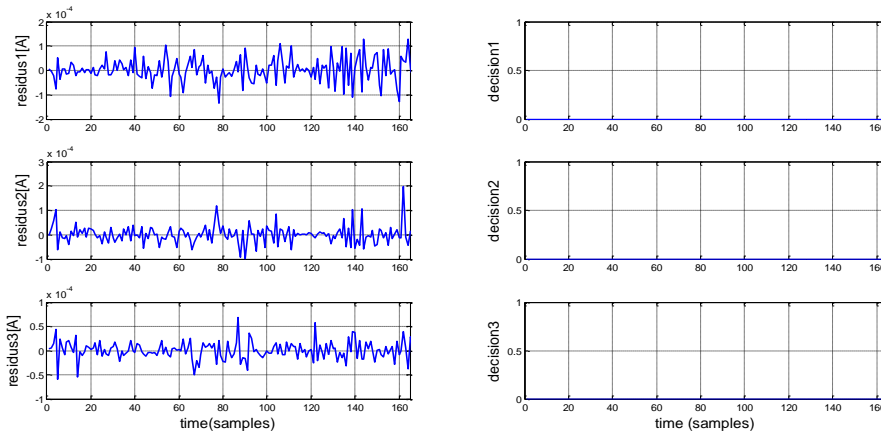


Figure 12. Identification residues and network decision: healthy case
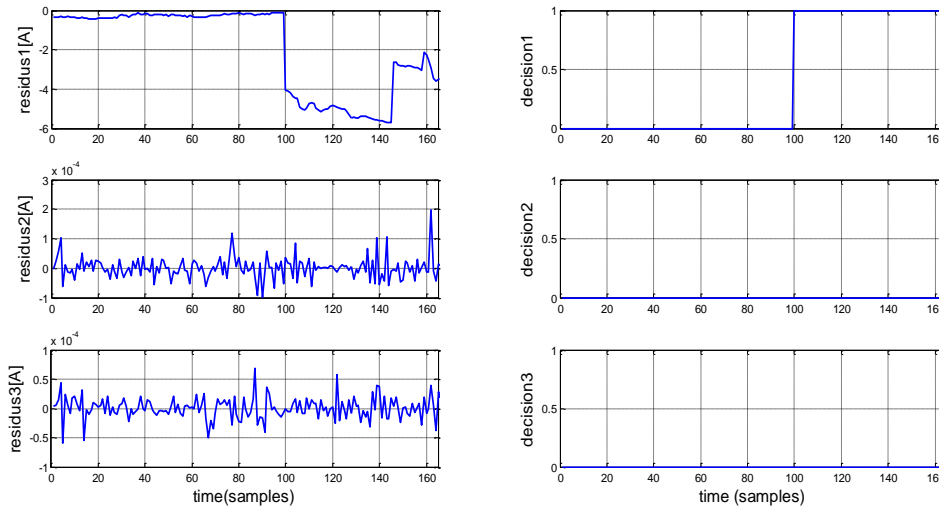


Figure 13. Network identification and decision residues: shunt default

- Case of shading phenomenon at string level III

Figure 15 presents the identification residues at the level of the three strings with the presence of the phenomenon of shading in the string III from the samples 50. The obtained identification residues show the effect of the presence of shading phenomenon on the residue of string III with an amplitude almost 9 A. This change corresponding to a logical response of network RNN is equal to 1 and zero in the others.

### 5.2.3. Combined fault case

In this part to show the sensitivity and the correct decision of our method of identification, we have introduced combined faults (shading + shunt) at the level of the strings of the PV system studied in different periods.
- Case of combined shading fault

Figure 16 shows the identification residues in the strings with the presence of shading defects at the string level I and II. The identification residues obtained show the effect of the shading phenomenon at the level of two strings I & II. According to the residues we see that the evolution of the residues in the presence of the shading phenomenon in the two strings is almost identical, which shows the robustness of our identification method.
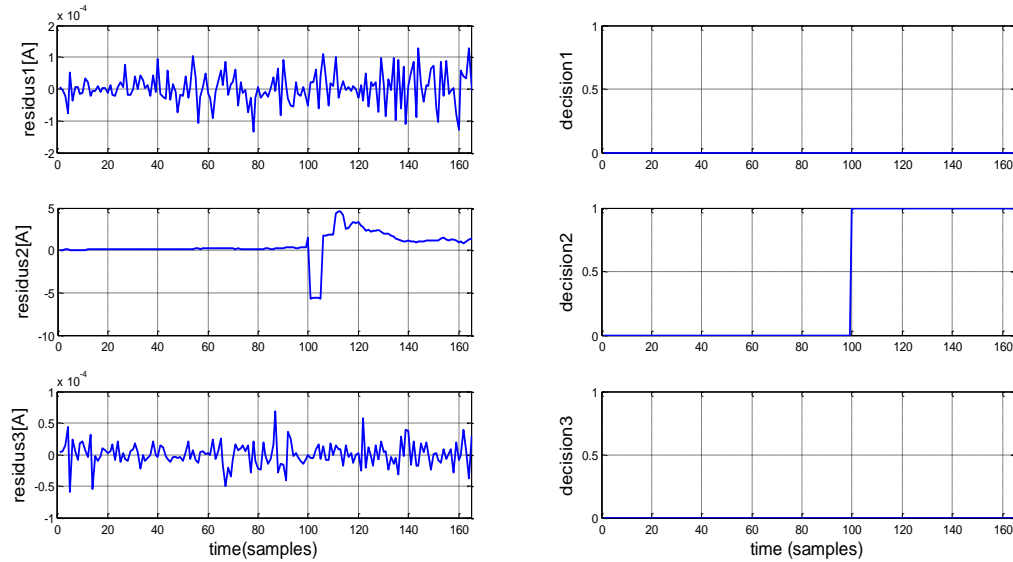


Figure 14. Network identification and decision residue: case of shading phenomenon
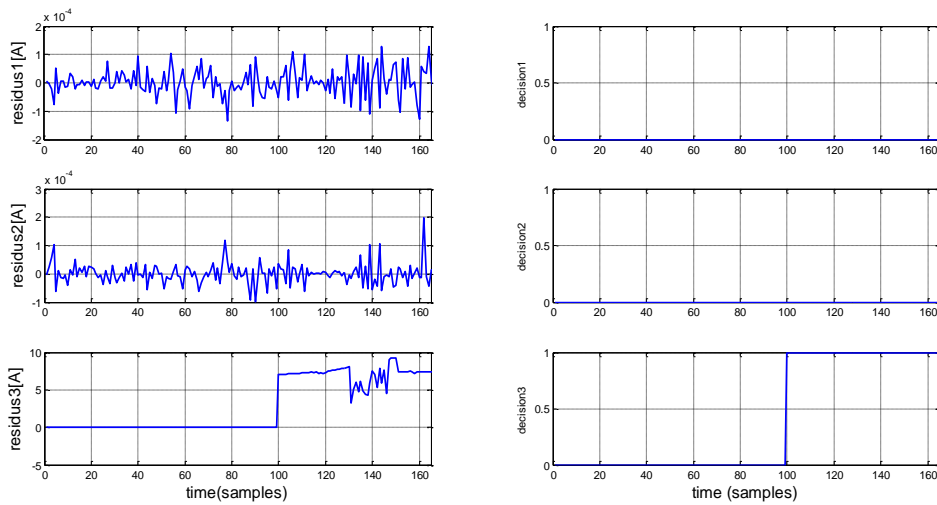


Figure 15. Network identification and decision residue: case of shading phenomenon

- Case of fault shunt and shading

Figure 17 presents the identification residues of the three strings of the PV system studied in the presence of a shunt fault at the string level I and the shading phenomenon at the string level II. The results obtained represent the effects of the defects on the identification residues, according to the two residues it is noted that, the residue of string I recorded by the sensor I reaches up to an amplitude of an absolute value of 5.7 A, and subsequently stabilizes with an absolute value of 4 A. In the same way the residue recorded by the sensor I at the level of string II reached at an amplitude of 4 A and stabilizes at a low value. The identification results illustrating the different faults are shown in the Table 3.
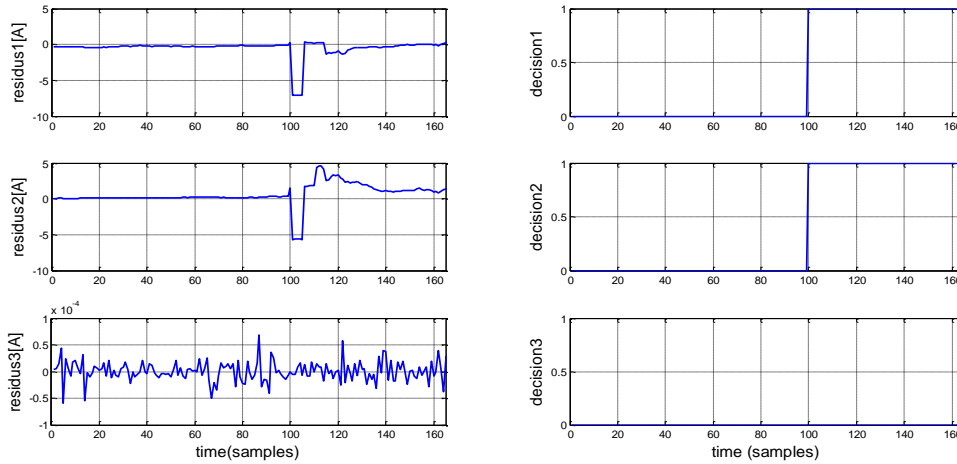
Figure 16. Network identification and decision residue: combined shading fault case
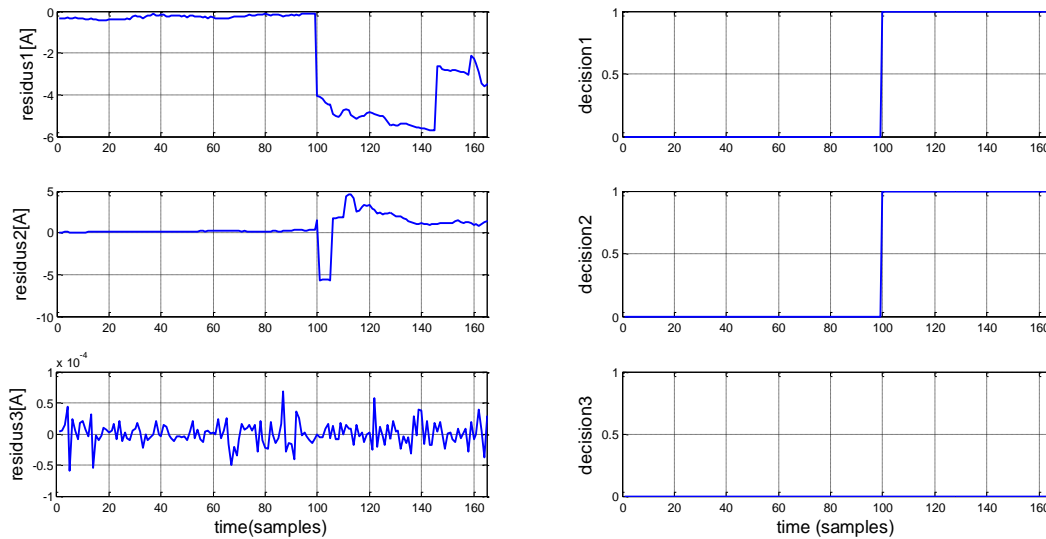


Figure 17. Network identification and decision residue: shunt fault and combined shading

Table 3. PV system fault identification

| States \ Decisions | | D1 | D2 | D3 |
|---|---|---|---|---|
| Normal states | | 0 | 0 | 0 |
| Simplefault | f1 | 1 | 0 | 0 |
| | f2 | 0 | 1 | 0 |
| | f3 | 0 | 0 | 1 |
| Combinefault | f4 | 1 | 1 | 0 |
| | f5 | 1 | 1 | 0 |

Where f1 is shunt fault at string level I; f2 is shading phenomenon at string level II; f3 is string level III shading phenomenon; f4 is combined shading fault at string level I & II; f5 is combined shunt & shading fault at string level I & II.

## 6.     CONCLUSION

The shunt faults and the phenomenon of shading generally presented the major problems in the PV systems, these problems influences the production of the electricity energies from the solar energies. In this

work we have developed modern approaches to detect and identify the shunt faults and the online shading phenomenon, the approach is developed based on the use of MLP type neural networks for the generation of PV system residues. At the strings, and another RNN type for the identification of physical faults. The obtained identification results show the precision and speed of the method developed to detect and identify physical defects in strings in the PV system. In the rest of this work, we will develop deep intelligent algorithms in order to diagnose and classify other faults in PV systems and apply them for more complicated systems such as multi-source renewable energy conversion systems.

## REFERENCES

[1] Z. Chen, L. Wu, S. Cheng, P. Lin, Y. Wu, and W. Lin, "Intelligent fault diagnosis of photovoltaic arrays based on optimized kernel extreme learning machine and I-V characteristics," *Applied Energy*, vol. 204, pp. 912–931, Oct. 2017, doi: 10.1016/j.apenergy.2017.05.034.

[2] L. Bouselham, M. Hajji, B. Hajji, and H. Bouali, "A new MPPT-based ANN for photovoltaic system under partial shading conditions," *Energy Procedia*, vol. 111, pp. 924–933, Mar. 2017, doi: 10.1016/j.egypro.2017.03.255.

[3] G. Chen, P. Lin, Y. Lai, Z. Chen, L. Wu, and S. Cheng, "Location for fault string of photovoltaic array based on current time series change detection," *Energy Procedia*, vol. 145, pp. 406–412, Jul. 2018, doi: 10.1016/j.egypro.2018.04.067.

[4] A. Belaout, F. Krim, A. Mellit, B. Talbi, and A. Arabi, "Multiclass adaptive neuro-fuzzy classifier and feature selection techniques for photovoltaic array fault detection and classification," *Renewable Energy*, vol. 127, pp. 548–558, Nov. 2018, doi: 10.1016/j.renene.2018.05.008.

[5] O. Hachana, G. M. Tina, and K. E. Hemsas, "PV array fault diagnostic technique for BIPV systems," *Energy and Buildings*, vol. 126, pp. 263–274, Aug. 2016, doi: 10.1016/j.enbuild.2016.05.031.

[6] S. Spataru, D. Sera, T. Kerekes, and R. Teodorescu, "Diagnostic method for photovoltaic systems based on light I–V measurements," *Solar Energy*, vol. 119, pp. 29–44, Sep. 2015, doi: 10.1016/j.solener.2015.06.020.

[7] M. H. Ali, A. Rabhi, A. E. Hajjaji, and G. M. Tina, "Real time fault detection in photovoltaic systems," *Energy Procedia*, vol. 111, pp. 914–923, Mar. 2017, doi: 10.1016/j.egypro.2017.03.254.

[8] W. Chine, A. Mellit, V. Lughi, A. Malek, G. Sulligoi, and A. M. Pavan, "A novel fault diagnosis technique for photovoltaic systems based on artificial neural networks," *Renewable Energy*, vol. 90, pp. 501–512, May 2016, doi: 10.1016/j.renene.2016.01.036.

[9] A. Mellit, S. Sağlam, and S. A. Kalogirou, "Artificial neural network-based model for estimating the produced power of a photovoltaic module," *Renewable Energy*, vol. 60, pp. 71–78, Dec. 2013, doi: 10.1016/j.renene.2013.04.011.

[10] A. Chouder and S. Silvestre, "Automatic supervision and fault detection of PV systems based on power losses analysis," *Energy Conversion and Management*, vol. 51, no. 10, pp. 1929–1937, Oct. 2010, doi: 10.1016/j.enconman.2010.02.025.

[11] D. Riley and J. Johnson, "Photovoltaic prognostics and heath management using learning algorithms," *in 2012 38th IEEE Photovoltaic Specialists Conference*, Jun. 2012, pp. 001535–001539, doi: 10.1109/PVSC.2012.6317887.

[12] E. Skoplaki and J. A. Palyvos, "On the temperature dependence of photovoltaic module electrical performance: a review of efficiency/power correlations," *Solar Energy*, vol. 83, no. 5, pp. 614–624, May 2009, doi: 10.1016/j.solener.2008.10.008.

[13] V. J. Chin, Z. Salam, and K. Ishaque, "Cell modelling and model parameters estimation techniques for photovoltaic simulator application: A review," *Applied Energy*, vol. 154, pp. 500–519, Sep. 2015, doi: 10.1016/j.apenergy.2015.05.035.

[14] K. Ishaque, Z. Salam, and H. Taheri, "Simple, fast and accurate two-diode model for photovoltaic modules," *Solar Energy Materials and Solar Cells*, vol. 95, no. 2, pp. 586–594, Feb. 2011, doi: 10.1016/j.solmat.2010.09.023.

[15] M. Davarifar, A. Rabhi, A. E. Hajjaji, and M. Dahmane, "New method for fault detection of PV panels in domestic applications," *in 3rd International Conference on Systems and Control*, Oct. 2013, pp. 727–732, doi: 10.1109/ICoSC.2013.6750940.

[16] A. Bouraiou, M. Hamouda, A. Chaker, M. Sadok, M. Mostefaoui, and S. Lachtar, "Modeling and simulation of photovoltaic module and array based on one and two diode model using matlab/simulink," *Energy Procedia*, vol. 74, pp. 864–877, Aug. 2015, doi: 10.1016/j.egypro.2015.07.822.

[17] M. Norgaard, O. Rav, N. K. Poulsen, and L. K. Hansen, "Neural networks for modelling and control of dynamic systems," in A Practitioner's Handbook, London: Springer, 2000, p. 246.

[18] O. Nelles, "Nonlinear Dynamic System Identification," in Nonlinear System Identification, Berlin, Heidelberg: Springer Berlin Heidelberg, 2001, pp. 547–577.

[19] M. Alexandru, C. Combastel, and S. Gentil, "Diagnostic decision using recurrent neural networks," *IFAC Proceedings Volumes*, vol. 33, no. 11, pp. 405–410, Jun. 2000, doi: 10.1016/S1474-6670(17)37392-5.

[20] M. L. Benloucif, "Neuro-fuzzy sensor fault diagnosis of an induction motor," *Journal of Engineering Research*, vol. 8, no. 1, pp. 53–60, 2011, doi: 10.24200/tjer.vol8iss1pp53-60.

[21] K. S. Narendra and K. Parthasarathy, "Identification and control of dynamical systems using neural networks," *IEEE Transactions on Neural Networks*, vol. 1, no. 1, pp. 4–27, Mar. 1990, doi: 10.1109/72.80202.

[22] Y. M. Chen and M. L. Lee, "Neural networks-based scheme for system failure detection and diagnosis," *Mathematics and Computers in Simulation*, vol. 58, no. 2, pp. 101–109, Jan. 2002, doi: 10.1016/S0378-4754(01)00330-5.

[23] Y. Kourd, N. Guersi and D. Lefebvre, "Neuro-fuzzy approach for default Diagnosis: Application to the DAMADICS," *4th IEEE International Conference on Digital Ecosystems and Technologies*, 2010, pp. 107-111, doi: 10.1109/DEST.2010.5610663.

[24] Ah Chung Tsoi and A. D. Back, "Locally recurrent globally feedforward networks: a critical review of architectures," *in IEEE Transactions on Neural Networks*, vol. 5, no. 2, pp. 229-239, March 1994, doi: 10.1109/72.279187.

[25] A. Evsukoff, C. Combastel, and S. Gentil, "Qualitative Reasoning and Neural Network Decision Procedures for Fault Detection and Isolation," *Proceedings of the 14th IFAC World Congress*, vol. 32, no. 2, pp. 7635-7640, 1994, doi: 10.1016/S1474-6670(17)57303-6.

## BIOGRAPHIES OF AUTHORS

**Reda Djeghader** [ID] [G] [SC] [O] was born on December 23, 1980 in Skikda, Algeria, He received his degrees of engineering and MSc. in automatic from University of Skikda, Algeria in 2004 and 2008 respectively and PhD in electromechanical. He is currently an associate professor at the University of Skikda, Algeria. His research interests are centered on diagnosis, renewable energy, and artificial neural networks. He can be contacted at email: r.djeghader@univ-skikda.dz.

**Ilyes Louahem Msabah** [ID] [G] [SC] [O] was born on February 5, 1995 in Skikda, Algeria. He received his degrees of Master in power system engineering from University of Boumerdes, Algeria in 2019 and PhD student in renewable energy. His research interests are centered on diagnosis and renewable energy. He can be contacted at email: i.louahemmsabah@univ-skikda.dz.

**Samia Benzahioul** [ID] [G] [SC] [O] was born on November 11, 1983 in Skikda, Algeria. She received his degrees of enginerring and MSc in 2010 and 2013 respectively and PhD in Electromechanical from University of Skikda in 2018. She is currently a professor at the University of Skikda, Algeria. Her research interests are centered on diagnosis, electrical machines, and renewable energy. She can be contacted at email: s.benzahioul@univ-skikda.dz.

**Abderrezak Metatla** [ID] [G] [SC] [O] was born on Februrary 18, 1977 in Skikda, Algeria. He received his degrees of enginerring and MSc. in 2004 and PhD in Electromechanical from University of Skikda in 2009 and professor in 2018. He is currently a professor at the University of Skikda, Algeria. His research interests are centered on diagnosis, electrical machines, and renewable energy. He can be contacted at email: a.metatla@univ-skikda.dz.